On demand and long-term drug delivery from degradable nanocapsules

Authors:

Sydney Menikheim[1]

Joshua Leckron[1]

Steven L. Bernstein[2]

Erin Lavik[1, *]

[1] Chemical, Biochemical, and Env. Eng. UMBC, Baltimore, MD 21250, Piscataway Territories

[2]Dept. of Ophthalmology and Visual Sciences, UMB, Baltimore, MD 21201

*corresponding author

Abstract

While there are a number of nanomaterials that can lead to on demand drug delivery or long-term delivery, there are limited nanotechnologies that are stable for long times, deliver sustained amounts of drugs, and achieve repeated, on demand delivery. We have developed a system based on polyurethane nanocapsules as a platform for long-term and on demand delivery. We synthesized nanocapsules encapsulating either a model drug, fluorescein, or a clinically relevant drug, acriflavine, a HIF-1alpha inhibitor. The nanocapsules were ~250 nm in diameter as measured by DLS and confirmed via SEM, and the molecules were localized in the walls of the nanocapsules as determined by confocal microscopy. Release studies were performed at 37 C in PBS, and both the fluorescein and acriflavine were delivered over several weeks. At the end of the release, no pellet was detectable upon centrifugation of the nanocapsules confirming degradation of the polyurethane shells. The same particles released a fraction of their payload upon the application of either an ultrasonic probe or a clinical grade, ultrasound imaging system used for assessing the retina. The amount of drug released could be tailored by the energy applied to the nanocapsules. One of the most exciting findings beyond being able to tailor how much was released based on the energy applied and the time it was applied was that these nanocapsules could be triggered to release multiple times with at least 10 separate release events triggered for each formulation. Being able to tailor the on-demand release over multiple cycles has the potential to fundamentally change how we can approach delivery of drugs for a variety of applications.

Graphical Abstract: TOC figure

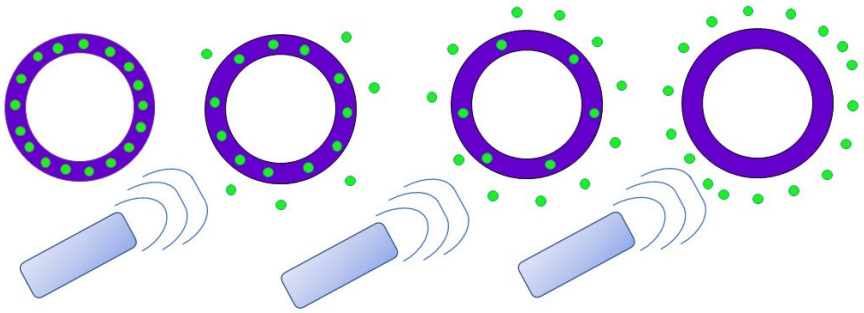

Nanocapsules containing drugs can be triggered to delivery on demand using a wide range of ultrasound frequencies and energies for many cycles leads to a long term, on demand delivery system.

Keywords

Keywords: sono, urethane, nanobubble, nanoparticle, ultrasound, age-related macular degeneration

On demand drug delivery has drawn a great deal of interest in recent years whether it is for targeted treatment of glioblastomas [1], delivering local anesthetics [2], or providing antibiotics [3]. These systems generally fall into two classes: nanomaterials that can be injected locally or systemically based on nanomaterials that are triggered by light or ultrasound [1, 4-6] or depots that are implanted into a location and, likewise, are generally triggered by light or sound [3, 7-8].

Depot systems can deliver molecules repeatedly in an on-demand fashion over long times. The majority of these depots require implantation, but once implanted can provide on-demand delivery over weeks [5, 7, 9]. Nanomaterial systems are generally used for one-time local delivery and, typically, are triggered shortly after administration. While investigations have utilized both light and sound, more studies have focused on ultrasound-triggered systems because of the ease with which ultrasound can be delivered to many locations in the body. Ultrasound triggered systems offer great potential for therapeutic delivery of a range of molecules on demand. The majority of work in this area has focused on micro- and nanobubbles based on liposomes, lipoplexes, and polymerosomes [10]. These are generally coated with albumin or lipoproteins for stability in blood [11]. While the majority of microbubble work has focused on contrast agents, studies evaluating delivery of therapeutics or combining therapeutics with contrast is growing rapidly [12].

The majority of studies evaluating drug delivery from these ultrasound-triggered systems have looked at local single timepoint delivery immediately after administration [11, 13-14]. Many of the formulations deliver their payload over minutes or hours post administration [15]. Stability of these systems is a concern. Considerable advances have occurred in both long term storage and improving stability of liposomal formulations [16-17]. Formulation is critically important. Gas encapsulated nanobubbles are not thermodynamically stable, but they can be engineered to be stable for hundreds of minutes by formulating their chemistry [18]. Microbubbles can be coated with nanoparticles which can be released from the bubbles by ultrasound [11]. This approach is similar to that of combining micro- or nanobubbles in promoting disruption of tight junctions, followed by delivery of nanoparticles where the nanoparticles then deliver the contents over time [14, 19-21]. While is a creative, combination approach, it does not address the need for long term delivery coupled with repeated on demand delivery. The nanoparticle aggregates have been developed that dissociate in the presence of ultrasound [22]. These particles can deliver their contents for days and weeks, but once triggered and delivered to the site, a tumor in this case, the delivery is passive [22]. The approach leads to more particles in the tumor compared to controls but does not address the desire for an on-demand system that can be used over time.

Multiple applications would benefit from an easily administered, on-demand system that combines the features of implantable depot systems with those of flexible nanoformulations. An ideal system would enable on-demand delivery over long times as well as be in a formulation that could be administered via multiple routes. In light of this need for materials that could permit long term delivery as well as addressable delivery, we sought to determine whether polyurethane nanocapsules could lead to long term delivery of a molecule that could also be triggered to release in higher amounts by ultrasound. As proof of principle, we encapsulated

fluorescein and looked at both the long term, passive delivery as well as ultrasound triggered release over multiple cycles over time. We then extended this work to include acriflavine, an anti-angiogenic compound with potential applications in age-related macular degeneration (AMD). Using our approach, we found that ultrasound triggered release in an on-demand manner many times and the amount delivered was a function of the ultrasound time. Finally, we showed that we could trigger release using a commercially available, clinically approved clinical-grade ultrasound system for ocular assessment.

Synthesis and Characterization of nanocapsules

Polyurethane nanocapsules encapsulating fluorescein were synthesized following [23-24]. Creating polyurethane nanocapsules using an interfacial polymerization process has a long history for a range of applications, but it has never been used to create an ultrasound triggered on demand delivery system. A schematic of the approach is shown in figure 1.

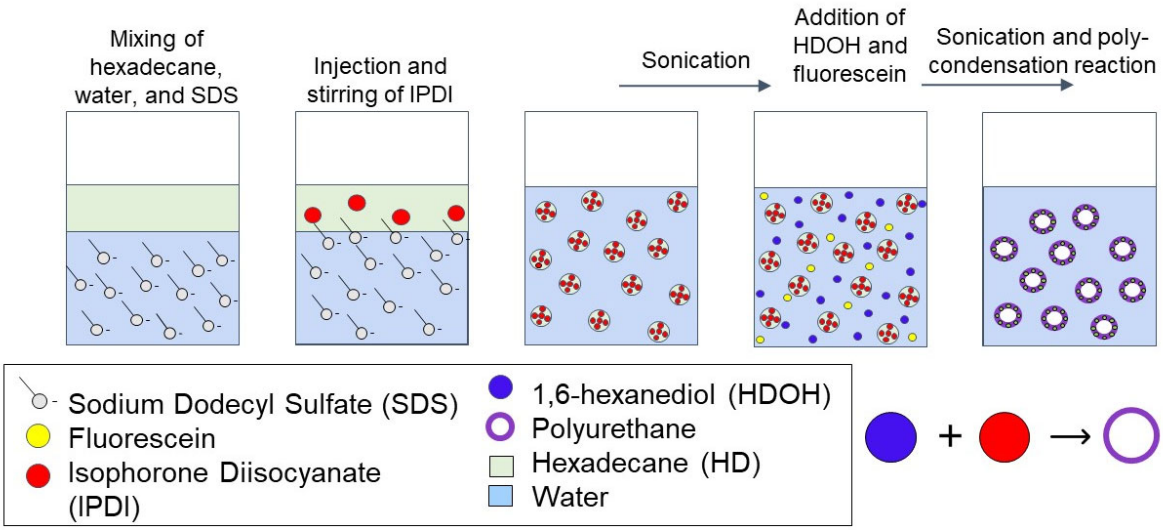

Figure 1. The synthesis method for the fluorescent capsule is depicted. Note that the SDS is a surfactant. It acts as a stabilizing agent and is always present; however, it is not be depicted fully in each step to avoid cluttering the image.

The FTIR spectrum (Fig 2A) demonstrates the successful synthesis of polyurethane in the nanocapules. The peak at 1550 cm-1 corresponds to the C-N vibration in the urethane and the peak at 1637 cm-1 is due to the urea carbonyl presence in the nanocapsules. The peak at 1720 cm-1 shows the C=O vibration, present in each capsule. Lastly, the peak at 3330 cm-1 corresponds to the N-H vibration [25-27]. Taken together, the interfacial polymerization led to the successful synthesis of polyurethane. Similar spectra were seen for both the fluorescein encapsulated nanocapsules and acriflavine nanocapsules. As one would expect with an interfacial polyermization of a polyurethane, the molecular weight of the polymer was low. Gel Permeation Chromatography showed an Mn~ 1,462 Da, and Mw~ 1,992 Da.

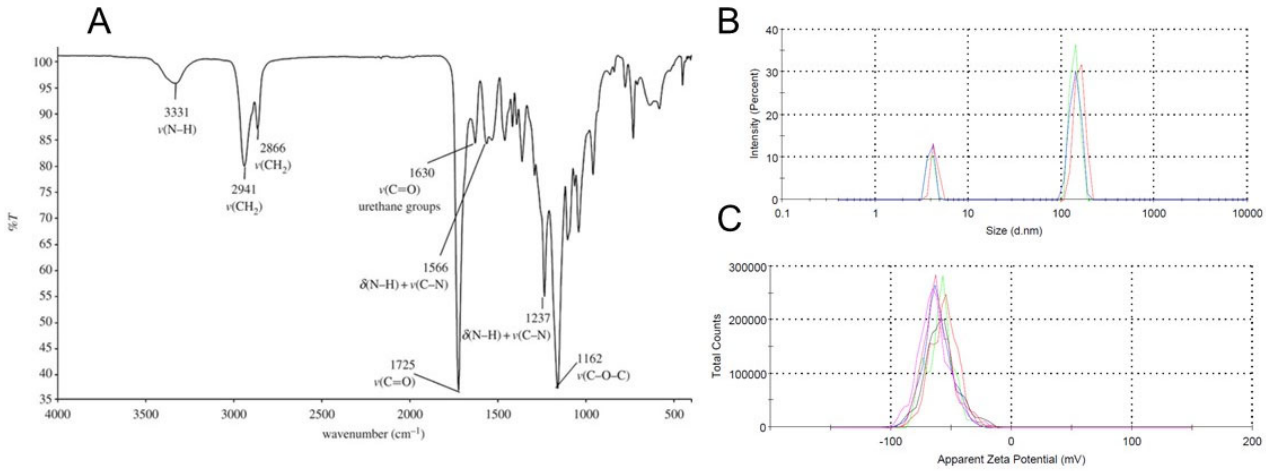

Figure 2: (A) FTIR spectra for the polyurethane nanocapsules encapsulating fluorescein showing the critical peaks at 1550 cm-1 (C-N vibration) 1637 cm-1 (urea carbonyl), 1720 cm-1 (C=O vibration) and 3330 cm-1 (N-H vibration). (B) DLS of polyurethane nanocapsules containing fluorescein shows two peaks with the larger peak, associated with the nanocapsules was 145+/-9 nm. (C) The zeta potential for the fluorescein nanocapsules was -60 mV+/- 12 mV.

The DLS showed two peaks with one close to 4 nm and the main one, correlated with the nanocapsules at 145+/-9 nm. The smaller peak is commonly seen in polyurethane syntheses [28-29]. The zeta potential is extremely negative (-60 mV+/- 12 mV) which is common with polyurethane-based materials made via emulsion polymerization both because of the carboxyls at the surface as well as the SDS used to form the emulsions [30-32].

Imaging of Nanocapsules

Scanning electron microscopy (SEM) was performed on nanocapsules before and after sonication studies. The SEM results correlated with the DLS findings with the fluorescein nanocapules being around 150 nm with a notable distribution in sizes. Many of the capsules looked partially deflated. We saw this is all batches and attribute it to the lyophilization of the nanocapsules. After sonication, we found that while there were some burst capsules, the majority remained intact. The post-sonication image in figure 3C is from the repeated 60 second sonication burst study (particles exposed to 1 minute sociation at 20 W with 10 repetitions) that led to the release curve in Figure 4C.

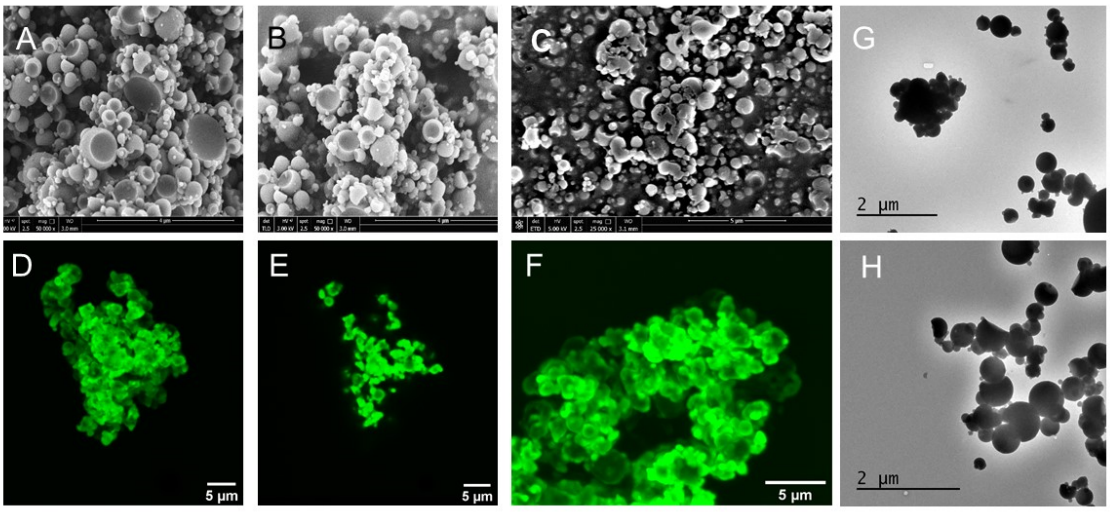

Figure 3: SEM micrographs and confocal images of fluorescein nanocapsules. (A) and (B) SEMs of fluorescein-containing nanocapsules which may be an artifact of the lyophilization process. (C) Post-sonication (repeated 60 second pluses leading to the data in fig. 4C), the majority of the particles are intact, but there are some fragments that can be seen in the image. (D-F) Confocal images of the nanocapsules showing that the fluorescein is localized in the shells of the nanocapsules. (G) TEM image of nanocapsules (H) TEM image of nanocapsules.

Confocal microscopy demonstrated that the fluorescein was localized in the shells of the nanocapsules. This is not surprising since fluorescein is a water-soluble molecule, and during the emulsification procedure, water-soluble molecules are likely to associate with the interfacial region of the nanoemulsion.

TEM of the nanocapsules showed a range of particle sizes consistent with the DLS data as well as some aggregates of nanocapsules (G) and individual nanocapsules (G and H). In the SEM, TEM, and confocal work, the nanocapsules look aggregated in places. We found that the dry nanocapsules often appeared aggregated but when resuspended, the particles dissociated. DLS was always performed after the particles had been lyophilized and then resuspended in ethanol or potassium chloride solution. For the confocal work, it was very difficult to resolve individual particles and we focused on the groupings since the primary purpose was to assess the localization of the drug.

Fluorescein release and on demand delivery

The loading of fluorescein was 0.012 ug of fluorescein per mg of nanocapsules. Based on the amounts initially added, the loading of the fluorescein was approximately 10% of the amount added. The amount was more than enough to investigate the passive release of fluorescein at 37°C from the nanocapsules versus the impact of sonication on release.

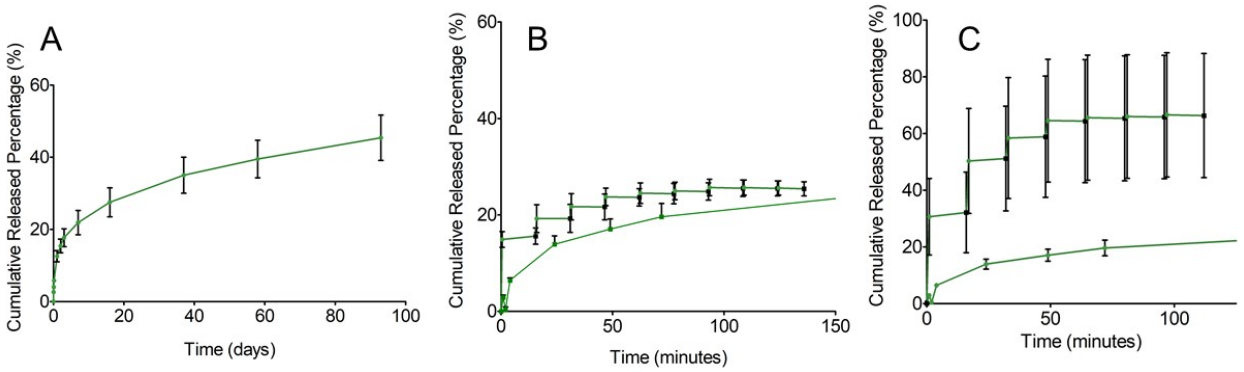

Figure 4: Release of fluorescein from nanocapsules. (A) Release of fluorescein from nanocapules using standard infinite sink model in PBS at 37 C. The long term delivery is replotted in B and C as a point of comparison. (B) Release from A overlaid by sonication time points. Samples were sonicated for 30 seconds at 15 minute intervals and the amount of fluorescein was measured at each time point. (C) Release from A overlaid by 60 second sonication events at 15 minute intervals.

Normal, passive delivery from the nanocapsules led to release of the fluorescein for over 90 days. At the end of 90 days, no capsules could be pelleted, and the release study was terminated. In all of our release studies carried to completion, the nanocapsules were degadaded to the point where no material could be collected. The synthesis of hexanediol with IPDI leads to urethane linkages, as confirmed by the FTIR in figure 1. Urethane linkages degrade either enzymatically [33-34] or by hydrolysis which is a significant limitation on using polyurethanes for long term applications in vivo, but it is a tremendous asset for a nanocapsule delivery system [35-37].

On demand delivery was achieve by exposing the nanocapsules to a sonicating probe device at 70% amplitude and 20 kHz which correlates with 20 Watts or 70W/cm^2 since we use a 6 mm probe. 30 second sonication events led to approximately 3-5% of the total amount of fluorescein being released. In contrast, 60 second sonication events led to ~25% of the fluorescein being released. This finding suggests one can tune the amount of a drug released by the amount of sonication applied over time. Having not only an on-demand system but an addressable on demand system could be extremely helpful in treating a number of conditions.

Acriflavine Long term release and on demand delivery

Based on the findings regarding fluorescein, we sought to apply this approach to a clinically relevant drug, acriflavine. Acriflavine was originally used as an antiseptic in WWII but has more recently been shown to be an effective inhibitor of HIF-1alpha dimerization and angiogenesis [38-39]. Acriflavine has been encapsulated previously in a lipid nanocapsule formulation for targeting tumors with the majority being released in the first four hours [40].

We encapsulated acriflavine in the polyurethane nanocapsules. The particles were 260+/-37 nm by DLS. The loading of the nanocapsules was 54 ug of acriflavine per mg of nanocapsules. This is well within the therapeutic window for delivery of acriflavine to inhibit angiogenesis [40-42].

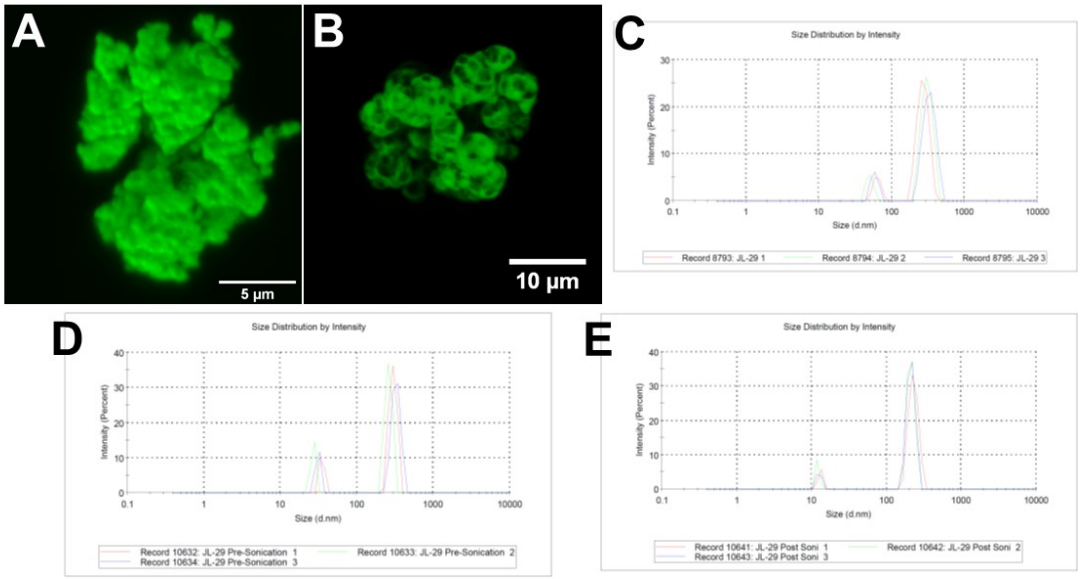

Figure 5: Confocal microscopy of acriflavine encapsulated nanocapsules. (A) Average Z-projection of the nanocapsules. (B) A slice through the nanocapsules showing the drug is localized in the shells of the nanocapsules. Like the fluorescein nanocapsules, acriflavine nanocapsules were far easier to visualize in clusters. C: DLS of the acriflavine nanocapsules post lyophilization have an average size of 330+/-63 nm. D: The nanocaspules were sized again prior to the sonication study and their average size was 295+/-33nm. E: These particles were exposed to 10 rounds of sonication for the data in figure 6, and then they were measured by DLS. Their post sonication size was 228+/-33 nm.

Acriflavine fluoresces with excitation at 416 nm and emission at 514 nm. We performed confocal microscopy and saw that the drug was localized in the shells of the nanocapsules as we had seen with fluorescein. As in the fluorescein nanocapsules, we visualized clusters of nanoparticles in the confocal microscope.

However, using DLS the nanocapule size was found to be 295+/-33nm with no signs of aggregates or large peaks. Following 10 rounds of sonication, the nanocapsules were the same dimensions by DLS. This all suggests that the nanocapsules are not aggregated in solution even after lyophilization and storage. It also suggests that they are remaining intact, as was seen with the fluorescein nanocapsules even after repeated sonications.

A standard infinite sink release was performed from the particles with approximately 10% being released over the first 5 weeks. (The release study was terminated after the 5th week due to the COVID-19 pandemic and the closing of the research lab.) Acriflavine is more hydrophobic than fluorescein which may account for the higher loading and slower release over time. The release curve for the acriflavine nanocapsules can be seen in figure 6A.

We then sonicated the nanocapsules using 20 second pulses at 30 minute intervals. The pulses consisted of 20 seconds of exposure to sonication at 50% amplitude, with a frequency of 20 kHz. The correlates with sonication at 10 Watts or 35 W/cm^2 based on probe dimensions. We found that this led to very tightly controlled, reproducible release of acriflavine at each sonication point with approximately 0.5 ug of acriflavine being released per mg of nanocapsules at each

sonication point. These sonication pulses were overlaid on the first part of the long term release curve to show the relative amount released over time in the absence and presence of sonication. Sonication leads to pulses of release of acriflavine.

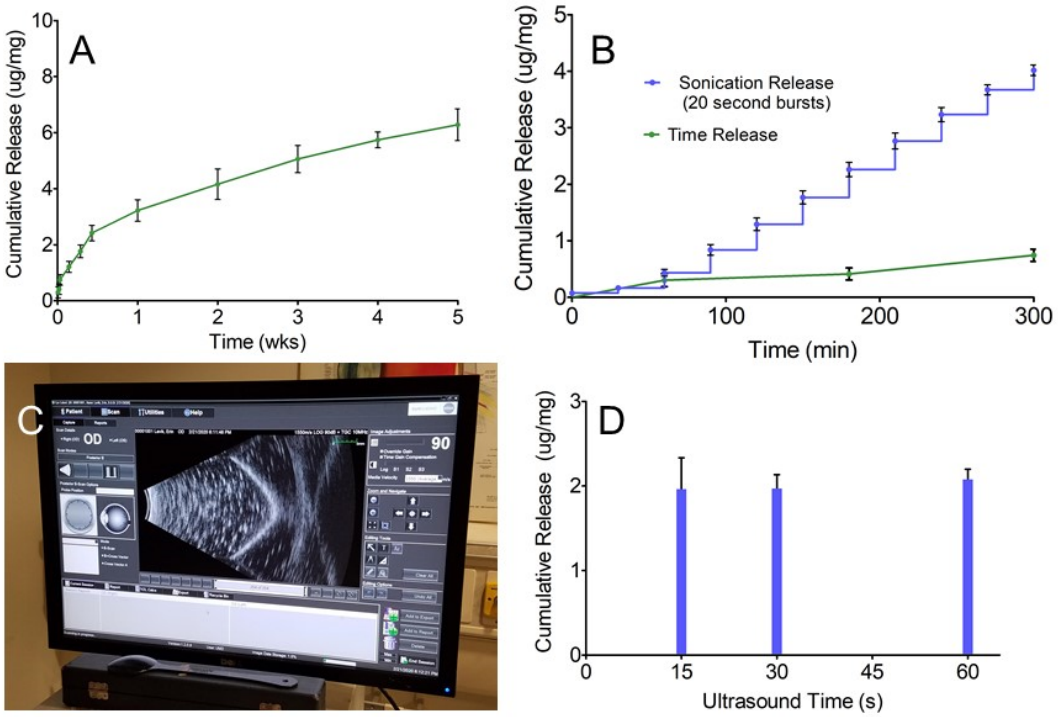

Figure 6: Delivery of acriflavine from nanocapsules. (A) Release curve for acriflavine nanocapsules (loading: 54 ug/mg nanocapsules). (B) Release curve overlaid with sonication release (via 20 second bursts) from acriflavine nanocapsules. The green curve is the first part of the long term release curve in (A). (C) Image of acriflavine nanocapsules in PBS in a 50 ml conical tube via the Ellex eyecubed ultrasound system. In the image, one can see the bottom of the 50 ml conical tube containing the nanocapsules which show bright signatures on the screen (D) Release of acriflavine from polyurethane nanocapsules exposed to ultrasound for different times at 90 dB and 10 MHz.

Being able to control the amount of drug released and being able to do so over 10 sonication steps over many hours is promising, but the question arose as to whether release could be controlled via a clinical instrument. The Ellex Eyecubed instrument (Ellex Corp). was used in the posterior B scan probe with the standard setting at 90 dB and 10 MHz. This setting is approved by the FDA for imaging the retina. The probe was placed into the solution with the nanocapsules and activated for 15, 30 or 60 seconds. Not surprisingly, the nanocapsules are bright on the ultrasound image with what appears to be high echogenicity much like their gas-containing microbubble counterparts [43-45]. Regardless of exposure time, the nanocapsules exhibited statistically similar release of approximately 2 ug of acriflavine per mg of nanocapsules. It is exciting that the nanocapsules can be seen by ultrasound. It is even more exciting that we can trigger on demand release even with an imaging setup, albeit at the highest setting and with the probe in the solution. The FDA limits the energy produced by clinical imaging probes to 0.72 W/cm^2 [46], so even a low energy system can trigger on demand release.

Polyurethane nanocapsules have been used extensively for self-healing dental resins and bone cements [27], essential oils [47] and enzymatically triggered drug delivery systems [48-49]. The last nanocapsules involve the incorporation of peptides into the polyurethane synthesis that are enzymatically degraded to trigger release in particular biological compartments. The novelty of our work is taking the concept of polyurethane nanocapsules and applying it to create a system that has both long term delivery as well as the ability to be able to deliver drugs on demand in a repeated fashion.

One of the important aspects of the polyurethane nanocapsules is that they can be lyophilized, stored, and resuspended just prior to use. All of the formulations studied here were lyophilized before either long term or on demand release studies were performed. Being able to lyophilize, store, and resuspend nanocapsules increased their ability to be deployed and used in a number of environments and applications.

We first performed the on-demand release using a sonicating probe. The fluorescein nanocapsules were sonicated at 20 kHz and 20 Watts or 70 W/cm^2 and the acriflavine nanocapsules were sonicated at 20 kHz and 10 Watts or 35 W/cm^2. These settings are consistent with high intensity focused ultrasound where the frequencies can be in the kilohertz range for tissue penetration and the power is often 100 W/cm^2 or higher [46]. In contrast, ultrasound for imaging is typically 2-3 MHz and limited to 0.72 W/cm^2 by the FDA [46]. Thus, it is particularly exciting that we were able to achieve release, albeit in vitro, with an FDA-approved ocular diagnostic imaging system. The B scan mode we used is 10 MHz which is optimized for viewing the retina. Higher frequencies have less penetration but greater resolution than lower frequencies, so ocular imaging systems use the high frequency ultrasound [50-51]. It is important to note that the low energy of a clinical imaging system suggests that these nanocapsules may be able to be used for drug delivery in spaces, such as the lung, where lower energies are needed for ultrasound to be safe and effective.

One of the outstanding questions is how does ultrasound trigger release of the drug in these systems. The two most likely possibilities are through hyperthermia and/or through cavitation [52]. While we will have to investigate this further, the early data over a wide range of energies and frequencies seems more consistent with cavitation than hyperthermia, but this remains to be determined conclusively in the future.

One huge attraction of current ultrasound-triggered systems is that they can be given intravenously [2, 53]. This current generation of polyurethane nanocapsules are not PEGylated or otherwise modified. Polyurethane nanoparticles have been used intravenously in a number of applications and appear to be cleared without issue [54]. There is always a concern with aggregation with any kind of nanomaterial as well as the potential for low circulation time, and particles in the current report can be easily PEGylated via the addition of an isocyanate functionalized PEG during the interfacial polymerization process [31, 54].

Nonetheless, not all polyurethane nanocapsules need to be delivered systemically to have a substantial biomedical impact. For a number of applications, an easily administered formulation that can deliver both a low level of a drug as well as a higher amount on demand may have substantial applications. One such example is the delivery of antiangiogenic molecules for AMD.

AMD is the leading cause of blindness in the United States [55-56]. While most of the patients exhibit non-neovascular dry AMD, 10-15% of AMD patients display an exudative form of the disease (wet AMD), associated with choroidal (subretinal) neovascular angiogenesis. This neovascularization is associated with subretinal fluid leakage, retinal scarring, and rapid vision loss [57]. Clinical therapies for wet AMD typically involve the intraocular delivery of antibodies or inhibitors to vascular endothelial growth factor (VEGF) as VEGF expression increases due to choroidal neovascularization in wet AMD [58]. Some of the anti-vascular endothelial growth factor (anti-VEGF) therapies that are currently used to treat AMD treatment include pegaptanib [59], ranibizumab [60-61], bevacizumab [60], and aflibercept [62], administered through intravitreal injections every four to six weeks. The ability to deliver a drug long times that could be triggered in the physician's office to tailor delivery, may greatly improve AMD treatment as a starting point. These nanocapsules have the potential to change the way we approach and treat diseases and provide a new ultrasound-triggered drug delivery platform.

Materials and Methods

Materials

All materials were obtained from commercial suppliers and used without further purification. Sodium dodecyl sulfate (SDS) (BP166, Fisher Scientific) and 99% pure hexadecane (AC120465000, ACROS Organics) were the surfactant and costabilizer, respectively, used to form the polyurethane nanocapsules. Isophorone diisocyanate (IPDI) 98% (AC427602500, ACROS Organics) and 1,6-hexanediol (HDOH) 97% (AAA1243930, ACROS Organics) were the reactants from which polyurethane was formed. Fluorescein (free acid, dye content 95%) (F2456, Sigma-Aldrich) was the fluorescent molecule that was encapsulated in the polyurethane shell and used to quantify the total mass that the polyurethane nanocapsules can encapsulate and release. Phosphate buffered solution (PBS) was used in the release study made via PBS tablets (P4417, MilliporeSigma).

Preparation of Fluorescein Nanocapsules

Polyurethane nanocapsules encapsulating fluorescein were synthesized referencing procedures previously published in literature to encapsulate triethylene glycol TEGDMA [23, 63]. Polyurethane nanocapsules were formed via a poly-condensation in a two-phase system through mini-emulsions. Again, hexadecane and DI water formed the two phases, an oil phase and an aqueous phase. SDS was used as the surfactant to confer colloidal stability [63].

Once 70 mL of water, 1.145 mL of hexadecane, and 1.1 g of surfactant (SDS) were mixed together at 300 rpm and 40°C for 1 hour, 2.094 mL of IPDI was slowly dripped into the mixture and stirred; this step began the synthesis of the nanocapsules. By dripping the IPDI and monomers into the solution, the IPDI was evenly distributed throughout the oil phase. As the IPDI solution entered the pre-emulsification solution, the stirring speed was increased to 400 rpm. Once the IPDI solution was fully injected into the beaker, the solution was mixed at 400 rpm and 40°C for 10 minutes. During this step, the solution remained clear. Next, the solution was sonicated with a 130-Watt Ultrasonic Processor with Thumb-actuated Pulser at an amplitude of 38% to break up any IPDI molecules that had aggregated. During this step,

emulsions formed, and the solution looked like milk. While sonication was still progressing, an aqueous solution of 0.0013 g of fluorescein and 5.9 g of HDOH and 10 mL of DI water was dripped into the system. Because of the high reactivity of the isocyanate, the IPDI reacted immediately with the HDOH at the interface of the two phases.[63].

After sonication, the solution was left to react for 24 hours at 40°C and mixing at 300 rpm. After 24 hours, much of the solvent had evaporated and a clear, viscous solution was left in the beaker. The solution was poured into a centrifuge tube and centrifuged with DI water for a total of 5 times at 10,000 rpm and 4 °C for 20 minutes each run. After each run, a distinct white pellet forms at the bottom of the tube. Additionally, after each run, the pale green supernatant was discarded, new DI water was added to the tube, and the pellet was resuspended. After the fifth centrifugation period, the supernatant was again discarded, new DI water was added, and the pellet was then resuspended. The resuspended pellet was frozen in liquid nitrogen, wrapped in aluminum foil to protect the particles from light exposure, and lyophilized. When fully dry, the capsules appeared to be a white powder.

Preparation of Acriflavine-releasing Polyurethane Nanocapsules

A 250 mL propylene beaker containing 1.1 g of sodium dodecyl sulfate (SDS) dissolved in 70 mL of DI water was prepared. This SDS and DI water solution was mixed with 1.145 mL of hexadecane, and the solution was allowed to stir at 40°C and 300 rpm for one hour. After an hour had passed, the stirring speed was raised to 400 rpm (with the temperature of 40 C being maintained) and 2.094 mL of IPDI mixed with 330 mg of acriflavine dissolved in 3-7 mL of DI water was added in dropwise to the beaker containing the DI water, SDS, and hexadecane. This dropwise addition was achieved by using a glass syringe attached to a 20 G needle. After the dropwise addition of the entirety of the acriflavine/IPDI/DI water solution under gravity was complete, the solution was allowed to stir for an additional 10 minutes at 400 rpm. The beaker and its contents were then transferred to a hood containing a sonicator. The solution was sonicated for one minute at 38% amplitude. After one minute, the solution continued to be sonicated at 38% amplitude while HDOH dissolved in 10 mL of DI water was added into the beaker over the course of one minute for a total of two minutes of cumulative sonication. Following sonication, the beaker and its contents were transferred back to a hot plate, and the reaction was allowed to occur at 40°C with a stirring speed of 300 rpm for 24 hours; this could be said to be a maturation step in which the IPDI and HDOH are allowed to react and form layers of polyurethane. During this step, the beaker was covered in aluminum foil to minimize light exposure.

Following the 24-hour maturation step, the formation of urethane had occurred. The urethane was found along the sides of the beaker as well as on the bottom of the beaker. What appears to be excess/unencapsulated acriflavine made some of the polyurethane appear a dark orange, while other urethane particles appeared light orange. All of the solid particles of urethane were transferred to a centrifuge tube and spun down for 10 minutes at 10,062x G. After centrifugation, a light orange pellet formed on the bottom and along the sides of the tube. Overtop of the pellet and the supernatant, a thin layer of hexadecane had formed, which was removed as completely as possible. Following removal of the hexadecane and the supernatant, enough fresh DI water was added to the tubes to cover the pellets. The DI water and pellet were

then vortexed briefly (for roughly ten seconds) and the solution was once again spun down at 10,062x G. The same process of removing the supernatant and hexadecane and adding new DI water was repeated, and the solution was spun down for a third and final time. After the third round of centrifugation, the hexadecane was often gone entirely, or present in small enough quantities to no longer be readily visible. The supernatant was removed once again, and the pellet of urethane was re-suspended in DI water. The suspension of urethane particles was then transferred to a pre-weighed 50 mL conical tube and was freeze-dried using liquid nitrogen. Following freeze-drying, the sample was wrapped in aluminum foil and lyophilized.

Characterization of Nanocapsules

Capsule morphology and size.

A vacuum sputter coater (Denton Desk II) was used to deposit a 20 nm layer of gold palladium onto the nanocapsule samples placed on carbon tape on a specimen stub for scanning electron microscopy (SEM) imaging using the Nova NanoSEM 450 from FEI. The surface morphology of the capsules was examined as well as the diameters of the capsules. Samples for transmission electron microscopy (TEM) were prepared by adding lyophilized particles to a carbon-coated copper grid. TEM was performed using a FEI Morgagni M268 100 kV TEM equipped with a Gatan Orius CCD camera.

Capsule size and zeta potential.

The Malvern ZetaSizer (Nano ZS90) was used to determine the diameter and calculated zeta potential of the nanocapsules via dynamic light scattering (DLS). The nanocapsules were placed in a 1mg/mL solution of 190 proof ethanol for sizing. This solution was pipetted into a cuvette (14955129, Fisher Scientific) which was placed into the ZetaSizer. The capsules were placed in a 1mg/mL solution of 10 mM potassium chloride (KCl) to determine the zeta potential. To measure the zeta potential, the solution was inserted into a folded capillary zeta cell (Malvern Store, DTS1070) which was placed in the ZetaSizer. Both the size and zeta potential measurements were run in triplicates.

Capsule molecular components and structures.

Fourier-transform infrared (FT-IR) (PerkinElmer Frontier Optica) spectroscopy was used to produce spectra to identify the molecular components and structures associated with the capsules.

Gel Permeation Chromatography

Gel Permeation Chromatography (GPC) (Viscotek, VE 2001) was used to measure the molecular weight and size of the components of the capsules. The GPC column (PL1110-6504) is of the Agilent Plgel MIXED family. Its phase is MIXED-D, its inner diameter is 7.5 mm, its length is 300 mm, and its particle size is 5 μm. To measure molecular weight and size, the reagents and capsule samples were first crushed via mortar and pestle. Then, a 10 mg of the crushed sample was resuspended in 1 mL of tetrahydrofuran (THF). This solution was filtered with PTFE membrane syringe filters (Fisher, 09-720-002) into GPC vials (VWR, 89239-024) which were placed in the machine for testing.

Characterization of Capsule Response to Sonication.

10 mg of the fluorescein capsules were suspended in PBS and the solution was sonicated with a 130-Watt Ultrasonic Processor with Thumb-actuated Pulser at an amplitude of 76% for 30 seconds. After sonication, the solution was centrifuged again, the supernatant was removed and measured on a fluorescent plate reader (Molecular Devices, SpectraMax M2) (excitation max: 485; emission max 525). New PBS was added to resuspend the pellet. Then, the solution was inserted into a rotator in an oven at 37°C for 15 minutes. After 15 minutes, the solution was again centrifuged, the supernatant was removed and tested, and new PBS was added to resuspend the pellet. The sonication and waiting were repeated until the fluorescent readings were unmeasureable. This entire process was repeated on another set of samples to determine the effect of the sonication time length. The only difference in this process was that the samples were sonicated at an amplitude of 76% for 1 minute. In between samples, the sonication probe was washed with acetone and dried off with a kimwipe or paper towel.

Sonication-Induced Release of Acriflavine Nanocapsules

10 mg of nanocapsules were placed in Eppendorf tubes with 1 ml of PBS. All experiments were performed in triplicate. The nanocapsules were exposed to 20 seconds of sonication at 50% amplitude. They were then centrifuged, the supernatant collected, and the pellet resuspended in fresh PBS. Samples were stored at -80 until they were read on the plate reader (excitation: 470 nm and emission: 513 nm). In between samples, the sonication probe was washed with acetone and dried off with a kimwipe or paper towel.

Characterization of Release of Drugs from Nanocapsules over Time

10 mg of the fluorescent capsules were suspended in PBS and the solution was placed in a rotator in an oven at 37°C. At specific time points, the solution was centrifuged for 10 minutes at 13.3 rpm, the supernatant was removed and stored in darkness at 4°C, and the pellet was resuspended in fresh PBS. The supernatant was then run on a fluorescent plate reader (Molecular Devices, SpectraMax M2) (excitation max: 490; emission max 525). This washing process was repeated until the optical density was below 20. At this point, the pellet was again resuspended in fresh PBS

Acriflavine release was performed in the same manner and the supernatant was measured on the plate reader excitation: 470 nm emission: 513 nm.

Ultrasound-Induced Release

The Eye cubed ultrasound imaging system (Ellex; Mawson Lakes, Australia) was used with the ocular probe in the B scan mode at 90 dB. 10 mg of acriflavine nanocapsules were added to 20 ml of PBS in 50 ml conical tubes. Three replicates were tested at each timepoint (15 second of ultrasound, 30 seconds of ultrasound, and 60 seconds of ultrasound.) The nanocapsules were held in PBS at room temperature for 90 minutes while getting access to the instrument. The probe was immersed in the solution for the designated time. Samples were then centrifuged, and the amount of acriflavine was determined using the SpectraMax M2 Microplate Reader (Molecular Devices LLC) in a 384-well Greiner black/clear plate. The excitation and emission wavelengths were 470 nm and 513 nm, respectively.

Acknowledgements

This work was supported by NIH grant 1R56NS100732-01. We would like to thank Samiha Sharlin, John Velkey and Grace Jones for assisting with fabrication and release studies, and Tagide deCarvalho, PhD and Sara Larson for assisting with confocal microscopy.

References

1. Luo, Z.; Jin, K.; Pang, Q.; Shen, S.; Yan, Z.; Jiang, T.; Zhu, X.; Yu, L.; Pang, Z.; Jiang, X., On-Demand Drug Release from Dual-Targeting Small Nanoparticles Triggered by High-Intensity Focused Ultrasound Enhanced Glioblastoma-Targeting Therapy. *ACS applied materials & interfaces* **2017,** *9* (37), 31612-31625.

2. Cullion, K.; Rwei, A. Y.; Kohane, D. S., Ultrasound-triggered liposomes for on-demand local anesthesia. *Ther Deliv* **2018,** *9* (1), 5-8.

3. Tamayol, A.; Hassani Najafabadi, A.; Mostafalu, P.; Yetisen, A. K.; Commotto, M.; Aldhahri, M.; Abdel-Wahab, M. S.; Najafabadi, Z. I.; Latifi, S.; Akbari, M.; Annabi, N.; Yun, S. H.; Memic, A.; Dokmeci, M. R.; Khademhosseini, A., Biodegradable elastic nanofibrous platforms with integrated flexible heaters for on-demand drug delivery. *Scientific reports* **2017,** *7* (1), 9220.

4. Li, J.; Sun, C.; Tao, W.; Cao, Z.; Qian, H.; Yang, X.; Wang, J., Photoinduced PEG deshielding from ROS-sensitive linkage-bridged block copolymer-based nanocarriers for on-demand drug delivery. *Biomaterials* **2018,** *170*, 147-155.

5. Lee, S.; Hwang, G.; Kim, T. H.; Kwon, S. J.; Kim, J. U.; Koh, K.; Park, B.; Hong, H.; Yu, K. J.; Chae, H.; Jung, Y.; Lee, J.; Kim, T. I., On-Demand Drug Release from Gold Nanoturf for a Thermo- and Chemotherapeutic Esophageal Stent. *ACS Nano* **2018,** *12* (7), 6756-6766.

6. Yuan, Z.; Demith, A.; Stoffel, R.; Zhang, Z.; Park, Y. C., Light-activated doxorubicin-encapsulated perfluorocarbon nanodroplets for on-demand drug delivery in an in vitro angiogenesis model: Comparison between perfluoropentane and perfluorohexane. *Colloids Surf B Biointerfaces* **2019,** *184*, 110484.

7. Lee, S. H.; Kim, B. H.; Park, C. G.; Lee, C.; Lim, B. Y.; Choy, Y. B., Implantable small device enabled with magnetic actuation for on-demand and pulsatile drug delivery. *J Control Release* **2018,** *286*, 224-230.

8. Brudno, Y.; Mooney, D. J., On-demand drug delivery from local depots. *J Control Release* **2015,** *219*, 8-17.

9. Khorshidi, S.; Karkhaneh, A., On-demand release of ciprofloxacin from a smart nanofiber depot with acoustic stimulus. *Journal of biosciences* **2018,** *43* (5), 959-967.

10. Ogawa, K.; Fuchigami, Y.; Hagimori, M.; Fumoto, S.; Maruyama, K.; Kawakami, S., Ultrasound-responsive nanobubble-mediated gene transfection in the cerebroventricular region

by intracerebroventricular administration in mice. *European journal of pharmaceutics and biopharmaceutics : official journal of Arbeitsgemeinschaft fur Pharmazeutische Verfahrenstechnik e.V* **2019,** *137*, 1-8.

11. Jamburidze, A.; Huerre, A.; Baresch, D.; Poulichet, V.; De Corato, M.; Garbin, V., Nanoparticle-Coated Microbubbles for Combined Ultrasound Imaging and Drug Delivery. *Langmuir : the ACS journal of surfaces and colloids* **2019,** *35* (31), 10087-10096.

12. Ma, J.; Xu, C. S.; Gao, F.; Chen, M.; Li, F.; Du, L. F., Diagnostic and therapeutic research on ultrasound microbubble/nanobubble contrast agents (Review). *Molecular medicine reports* **2015,** *12* (3), 4022-4028.

13. Wu, M.; Zhao, H.; Guo, L.; Wang, Y.; Song, J.; Zhao, X.; Li, C.; Hao, L.; Wang, D.; Tang, J., Ultrasound-mediated nanobubble destruction (UMND) facilitates the delivery of A10-3.2 aptamer targeted and siRNA-loaded cationic nanobubbles for therapy of prostate cancer. *Drug delivery* **2018,** *25* (1), 226-240.

14. Huang, D.; Chen, Y.-S.; Thakur, S. S.; Rupenthal, I. D., Ultrasound-mediated nanoparticle delivery across ex vivo bovine retina after intravitreal injection. *European journal of pharmaceutics and biopharmaceutics : official journal of Arbeitsgemeinschaft fur Pharmazeutische Verfahrenstechnik e.V* **2017,** *119*, 125-136.

15. Song, Z.; Wang, Z.; Shen, J.; Xu, S.; Hu, Z., Nerve growth factor delivery by ultrasound-mediated nanobubble destruction as a treatment for acute spinal cord injury in rats. *International journal of nanomedicine* **2017,** *12*, 1717-1729.

16. Simões, M. G.; Hugo, A.; Alves, P.; Pérez, P. F.; Gómez-Zavaglia, A.; Simões, P. N., Long term stability and interaction with epithelial cells of freeze-dried pH-responsive liposomes functionalized with cholesterol-poly(acrylic acid). *Colloids and surfaces. B, Biointerfaces* **2018,** *164*, 50-57.

17. Payton, N. M.; Wempe, M. F.; Xu, Y.; Anchordoquy, T. J., Long-term storage of lyophilized liposomal formulations. *Journal of pharmaceutical sciences* **2014,** *103* (12), 3869-3878.

18. Hernandez, C.; Nieves, L.; de Leon, A. C.; Advincula, R.; Exner, A. A., Role of Surface Tension in Gas Nanobubble Stability Under Ultrasound. *ACS applied materials & interfaces* **2018,** *10* (12), 9949-9956.

19. Husseini, G. A.; Pitt, W. G.; Martins, A. M., Ultrasonically triggered drug delivery: breaking the barrier. *Colloids and surfaces. B, Biointerfaces* **2014,** *123*, 364-386.

20. Baghirov, H.; Snipstad, S.; Sulheim, E.; Berg, S.; Hansen, R.; Thorsen, F.; Mørch, Y.; Davies, C. d. L.; Åslund, A. K. O., Ultrasound-mediated delivery and distribution of polymeric nanoparticles in the normal brain parenchyma of a metastatic brain tumour model. *PloS one* **2018,** *13* (1), e0191102-e0191102.

21. Ye, D.; Zhang, X.; Yue, Y.; Raliya, R.; Biswas, P.; Taylor, S.; Tai, Y.-C.; Rubin, J. B.; Liu, Y.; Chen, H., Focused ultrasound combined with microbubble-mediated intranasal delivery of gold nanoclusters to the brain. *Journal of controlled release : official journal of the Controlled Release Society* **2018,** *286*, 145-153.

22. Papa, A.-L.; Korin, N.; Kanapathipillai, M.; Mammoto, A.; Mammoto, T.; Jiang, A.; Mannix, R.; Uzun, O.; Johnson, C.; Bhatta, D.; Cuneo, G.; Ingber, D. E., Ultrasound-sensitive nanoparticle aggregates for targeted drug delivery. *Biomaterials* **2017,** *139*, 187-194.

23. Torini, L.; Argillier, J. F.; Zydowicz, N., Interfacial Polycondensation Encapsulation in Miniemulsion. *Macromolecules* **2005,** *38* (8), 3225-3236.

24. GUO Jinxin, P. Q., HUANG Cui, ZHAO Yanbing, OUYANG Xiaobai, HUO Yonghong, and DUAN Sansan, The Role of Surfactant and Costabilizer in Controlling Size of Nanocapsules Containing TEGDMA in Miniemulsion. **2009,** *24* (6).

25. Hung, W. C.; Shau, M. D.; Kao, H. C.; Shih, M. F.; Cherng, J. Y., The synthesis of cationic polyurethanes to study the effect of amines and structures on their DNA transfection potential. *Journal of Controlled Release* **2009,** *133* (1), 68-76.

26. Sobczak, M., Synthesis and Characterization of Polyurethanes Based on Oligo(ϵ-caprolactone) Prepared by Free-Metal Method. *Journal of Macromolecular Science, Part A* **2011,** *48* (5), 373-380.

27. Ouyang, X.; Huang, X.; Pan, Q.; Zuo, C.; Huang, C.; Yang, X.; Zhao, Y., Synthesis and characterization of triethylene glycol dimethacrylate nanocapsules used in a self-healing bonding resin. *Journal of dentistry* **2011,** *39* (12), 825-33.

28. Su, J. F.; Wang, L. X.; Ren, L.; Huang, Z.; Meng, X. W., Preparation and characterization of polyurethane microcapsules containing n-octadecane with styrene-maleic anhydride as a surfactant by interfacial polycondensation. *Journal of Applied Polymer Science* **2006,** *102* (5), 4996-5006.

29. Wu, J.; Weir, M. D.; Zhang, Q.; Zhou, C.; Melo, M. A. S.; Xu, H. H. K., Novel self-healing dental resin with microcapsules of polymerizable triethylene glycol dimethacrylate and N,N-dihydroxyethyl-p-toluidine. *Dental materials : official publication of the Academy of Dental Materials* **2016,** *32* (2), 294-304.

30. Zhu, Q.; Wang, Y.; Zhou, M.; Mao, C.; Huang, X.; Bao, J.; Shen, J., Preparation of anionic polyurethane nanoparticles and blood compatible behaviors. *J Nanosci Nanotechnol* **2012,** *12* (5), 4051-6.

31. Pabari, R. M.; Mattu, C.; Partheeban, S.; Almarhoon, A.; Boffito, M.; Ciardelli, G.; Ramtoola, Z., Novel polyurethane-based nanoparticles of infliximab to reduce inflammation in an in-vitro intestinal epithelial barrier model. *Int J Pharm* **2019,** *565*, 533-542.

32. Huang, Y. J.; Hung, K. C.; Hsieh, F. Y.; Hsu, S. H., Carboxyl-functionalized polyurethane nanoparticles with immunosuppressive properties as a new type of anti-inflammatory platform. *Nanoscale* **2015,** *7* (48), 20352-64.

33. Tang, Y. W.; Labow, R. S.; Santerre, J. P., Enzyme-induced biodegradation of polycarbonate-polyurethanes: Dependence on hard-segment chemistry. *Journal of Biomedical Materials Research* **2001,** *57* (4), 597-611.

34. Kreitz, M. R.; Domm, J. A.; Mathiowitz, E., Controlled delivery of therapeutics from microporous membranes. II. In vitro degradation and release of heparin-loaded poly(D,L-lactide-co-glycolide). *Biomaterials* **1997,** *18* (24), 1645-51.

35. Żółtowska, K.; Piotrowska, U.; Oledzka, E.; Kuras, M.; Zgadzaj, A.; Sobczak, M., Biodegradable Poly(ester-urethane) Carriers Exhibiting Controlled Release of Epirubicin. *Pharm Res* **2017,** *34* (4), 780-792.

36. Aluri, R.; Saxena, S.; Joshi, D. C.; Jayakannan, M., Multistimuli-Responsive Amphiphilic Poly(ester-urethane) Nanoassemblies Based on l-Tyrosine for Intracellular Drug Delivery to Cancer Cells. *Biomacromolecules* **2018,** *19* (6), 2166-2181.

37. Chaffin, K. A.; Chen, X.; McNamara, L.; Bates, F. S.; Hillmyer, M. A., Polyether Urethane Hydrolytic Stability after Exposure to Deoxygenated Water. *Macromolecules* **2014,** *47* (15), 5220-5226.

38. Zeng, M.; Shen, J.; Liu, Y.; Lu, L. Y.; Ding, K.; Fortmann, S. D.; Khan, M.; Wang, J.; Hackett, S. F.; Semenza, G. L.; Campochiaro, P. A., The HIF-1 antagonist acriflavine: visualization in retina and suppression of ocular neovascularization. *J Mol Med (Berl)* **2017,** *95* (4), 417-429.

39. Lee, K.; Zhang, H.; Qian, D. Z.; Rey, S.; Liu, J. O.; Semenza, G. L., Acriflavine inhibits HIF-1 dimerization, tumor growth, and vascularization. *Proc Natl Acad Sci U S A* **2009,** *106* (42), 17910-5.

40. Montigaud, Y.; Ucakar, B.; Krishnamachary, B.; Bhujwalla, Z. M.; Feron, O.; Préat, V.; Danhier, F.; Gallez, B.; Danhier, P., Optimized acriflavine-loaded lipid nanocapsules as a safe and effective delivery system to treat breast cancer. *Int J Pharm* **2018,** *551* (1-2), 322-328.

41. Lian, G.; Li, X.; Zhang, L.; Zhang, Y.; Sun, L.; Zhang, X.; Liu, H.; Pang, Y.; Kong, W.; Zhang, T.; Wang, X.; Jiang, C., Macrophage metabolic reprogramming aggravates aortic dissection through the HIF1α-ADAM17 pathway(☆). *EBioMedicine* **2019,** *49*, 291-304.

42. Cheloni, G.; Tanturli, M.; Tusa, I.; Ho DeSouza, N.; Shan, Y.; Gozzini, A.; Mazurier, F.; Rovida, E.; Li, S.; Dello Sbarba, P., Targeting chronic myeloid leukemia stem cells with the hypoxia-inducible factor inhibitor acriflavine. *Blood* **2017,** *130* (5), 655-665.

43. Picheth, G.; Houvenagel, S.; Dejean, C.; Couture, O.; Alves de Freitas, R.; Moine, L.; Tsapis, N., Echogenicity enhancement by end-fluorinated polylactide perfluorohexane nanocapsules: Towards ultrasound-activable nanosystems. *Acta Biomater* **2017,** *64*, 313-322.

44. Houvenagel, S.; Moine, L.; Picheth, G.; Dejean, C.; Brûlet, A.; Chennevière, A.; Faugeras, V.; Huang, N.; Couture, O.; Tsapis, N., Comb-Like Fluorophilic-Lipophilic-Hydrophilic Polymers for Nanocapsules as Ultrasound Contrast Agents. *Biomacromolecules* **2018,** *19* (8), 3244-3256.

45. Achmad, A.; Yamaguchi, A.; Hanaoka, H.; Tsushima, Y., Thin-Shelled PEGylated Perfluorooctyl Bromide Nanocapsules for Tumor-Targeted Ultrasound Contrast Agent. *Contrast media & molecular imaging* **2018,** *2018*, 1725323.

46. Phenix, C. P.; Togtema, M.; Pichardo, S.; Zehbe, I.; Curiel, L., High intensity focused ultrasound technology, its scope and applications in therapy and drug delivery. *Journal of pharmacy & pharmaceutical sciences : a publication of the Canadian Society for Pharmaceutical Sciences, Societe canadienne des sciences pharmaceutiques* **2014,** *17* (1), 136-53.

47. Cui, G.; Wang, J.; Wang, X.; Li, W.; Zhang, X., Preparation and Properties of Narrowly Dispersed Polyurethane Nanocapsules Containing Essential Oil via Phase Inversion Emulsification. *Journal of agricultural and food chemistry* **2018,** *66* (41), 10799-10807.

48. Andrieu, J.; Kotman, N.; Maier, M.; Mailänder, V.; Strauss, W. S.; Weiss, C. K.; Landfester, K., Live monitoring of cargo release from peptide-based hybrid nanocapsules induced by enzyme cleavage. *Macromolecular rapid communications* **2012,** *33* (3), 248-53.

49. Pramanik, S. K.; Sreedharan, S.; Singh, H.; Khan, M.; Tiwari, K.; Shiras, A.; Smythe, C.; Thomas, J. A.; Das, A., Mitochondria Targeting Non-Isocyanate-Based Polyurethane Nanocapsules for Enzyme-Triggered Drug Release. *Bioconjug Chem* **2018,** *29* (11), 3532-3543.

50. Powers, J.; Kremkau, F., Medical ultrasound systems. *Interface focus* **2011,** *1* (4), 477-89.

51. Jensen, J. A., Medical ultrasound imaging. *Progress in biophysics and molecular biology* **2007,** *93* (1-3), 153-65.

52. Sirsi, S. R.; Borden, M. A., State-of-the-art materials for ultrasound-triggered drug delivery. *Adv Drug Deliv Rev* **2014,** *72*, 3-14.

53. Xu, J.; Tu, H.; Ao, Z.; Chen, Y.; Danehy, R.; Guo, F., Acoustic disruption of tumor endothelium and on-demand drug delivery for cancer chemotherapy. *Nanotechnology* **2019,** *30* (15), 154001.

54. Rocas, P.; Fernández, Y.; García-Aranda, N.; Foradada, L.; Calvo, P.; Avilés, P.; Guillén, M. J.; Schwartz, S., Jr.; Rocas, J.; Albericio, F.; Abasolo, I., Improved pharmacokinetic profile of lipophilic anti-cancer drugs using αvβ3-targeted polyurethane-polyurea nanoparticles. *Nanomedicine* **2018,** *14* (2), 257-267.

55. da Cruz, L.; Fynes, K.; Georgiadis, O.; Kerby, J.; Luo, Y. H.; Ahmado, A.; Vernon, A.; Daniels, J. T.; Nommiste, B.; Hasan, S. M.; Gooljar, S. B.; Carr, A. F.; Vugler, A.; Ramsden, C. M.; Bictash, M.; Fenster, M.; Steer, J.; Harbinson, T.; Wilbrey, A.; Tufail, A.; Feng, G.; Whitlock, M.; Robson, A. G.; Holder, G. E.; Sagoo, M. S.; Loudon, P. T.; Whiting, P.; Coffey, P. J., Phase 1 clinical study of an embryonic stem cell-derived retinal pigment epithelium patch in age-related macular degeneration. *Nat Biotechnol* **2018,** *36* (4), 328-337.

56. Kamao, H., Preclinical Study of Human Induced Pluripotent Stem Cell-derived Retinal Pigment Epithelium Cell Sheets Transplantation. *Nippon Ganka Gakkai zasshi* **2016,** *120* (11), 754-63.

57. Ambati, J.; Fowler, B. J., Mechanisms of age-related macular degeneration. *Neuron* **2012,** *75* (1), 26-39.

58. Spilsbury, K.; Garrett, K. L.; Shen, W. Y.; Constable, I. J.; Rakoczy, P. E., Overexpression of vascular endothelial growth factor (VEGF) in the retinal pigment epithelium leads to the development of choroidal neovascularization. *Am J Pathol* **2000,** *157* (1), 135-44.

59. Gragoudas, E. S.; Adamis, A. P.; Cunningham, E. T., Jr.; Feinsod, M.; Guyer, D. R., Pegaptanib for neovascular age-related macular degeneration. *N Engl J Med* **2004,** *351* (27), 2805-16.

60. Martin, D. F.; Maguire, M. G.; Ying, G. S.; Grunwald, J. E.; Fine, S. L.; Jaffe, G. J., Ranibizumab and bevacizumab for neovascular age-related macular degeneration. *N Engl J Med* **2011,** *364* (20), 1897-908.

61. Rosenfeld, P. J.; Rich, R. M.; Lalwani, G. A., Ranibizumab: Phase III clinical trial results. *Ophthalmology clinics of North America* **2006,** *19* (3), 361-72.

62. Semeraro, F.; Morescalchi, F.; Duse, S.; Parmeggiani, F.; Gambicorti, E.; Costagliola, C., Aflibercept in wet AMD: specific role and optimal use. *Drug design, development and therapy* **2013,** *7*, 711-22.

63. Guo, J.; Pan, Q.; Huang, C.; Zhao, Y.; Ouyang, X.; Huo, Y.; Duan, S., The role of surfactant and costabilizer in controlling size of nanocapsules containing TEGDMA in miniemulsion. *Journal of Wuhan University of Technology-Mater. Sci. Ed.* **2009,** *24* (6), 1004.